Charge Density and Experimental Electrostatic Potentials of Two Penicillin Derivatives

Armin Wagner,[a, c] Ralf Flaig,[b] Birger Dittrich,[a] Horst Schmidt,[d] Tibor Koritsánszky,[e] and Peter Luger*[a]

Abstract: Two penicillin derivatives, the active penamecillin and the inactive penamecillin-1β-sulfoxide, were used to study the relationship between their charge density and their activity. Single crystals of both compounds were measured at the synchrotron beamline F1 at the HASYLAB/DESY, at 100 K and up to resolutions of around 0.4 Å. Experimental charge densities were obtained by using the Hansen–Coppens multipole formalism. The cleavage of the amide bond in the β-lactam ring is of paramount importance in the mechanism of action of penicillins. Topological analysis of this bond in terms of Bader's AIM theory showed that its strength is equal in both compounds; therefore a direct influence of bond strength on the activity can be ruled out. However, the two derivatives differ significantly in their experimental electrostatic potentials. These differences are discussed and provide further insight into the chemistry and activity of penicillins.

Keywords: charge density · electronic structure · penicillin · X-ray diffraction

Introduction

The number of experimental charge-density studies, especially on larger molecules,[1–4] has increased considerably during the last few years. This is due to technical developments, in particular, the now widely available area detectors which allow the measurement of high-resolution X-ray diffraction data sets within a reasonable time period. The combination of the area-detection technique with a high-intensity primary beam provided by synchrotron sources opens up the method to applications on compounds of biological relevance.[5]

[a] Dr. A. Wagner, Dr. B. Dittrich, Prof. Dr. P. Luger
Institut für Chemie/Kristallographie, Freie Universität Berlin
Takustrasse 6, 14195 Berlin (Germany)
Fax: (+49) 30-83853464
E-mail: luger@chemie.fu-berlin.de

[b] Dr. R. Flaig
Laboratoire de Biologie et Génomique Structurales de l'IGBMC
1 rue Laurent Fries, B.P. 10142, 67404 Illkirch Cedex (France)

[c] Dr. A. Wagner
Paul Scherrer Institut, Swiss Light Source
WSLA/220, 5232 Villigen PSI (Switzerland)

[d] Dr. H. Schmidt
Mineralogisch–Petrographisches Institut, Universität Hamburg
Grindelallee 48, 20146 Hamburg (Germany)

[e] Prof. Dr. T. Koritsánszky
Department of Chemistry, Middle Tennessee State University
P.O. Box 68, Murfreesboro, TN 37132 (USA)

Penicillins are among the most widely used antibiotics. Their antibacterial activity is based on preventing the synthesis of the bacterial cell wall by inhibiting the D-alanyl-D-alanine-transpeptidase. This enzyme cross-links terminal D-alanine residues of small peptides with glycine residues of the peptidoglycan, which is the integral part of the bacterial cell wall. Penicillins can be seen as substrate analogues of D-alanyl-D-alanine. By opening the β-lactam ring they irreversibly bind the active center of the D-alanyl-D-alanine-transpeptidase.[6]

Structure–activity-relationship studies for penicillins and other β-lactam antibiotics have suggested quite controversial models. The conventional interpretation relates the activity to the instability of the amide bond in the β-lactam ring;[7] the weaker this bond is the more electrophilic the carbonyl carbon atom is. There are two reasons that explain why the amide bond of the lactam is expected to be weaker than in a normal peptide bond: 1) the lactam ring is highly strained and 2) the lack of resonance of the bond; this is also due to steric effects because the planarity accompanied by the delocalization of the nitrogen atom's lone pair would require the thiazolidine ring to be coplanar with the lactam ring. The conformation of the bicyclic ring system therefore seems to be of central importance for activity, although there are examples of active antibiotics in different conformations.[8,9] This suggests that the actual conformation adopted by the penicillin substrate is altered upon binding to the enzyme. Indeed, recent diffraction studies show that the thiazolidine ring in penicillin G adopts a conformation

 DOI: 10.1002/chem.200305627

in the cleavage site of the acylase that is considerably different from that found in the crystal structure of the parent molecule.[10] This change in ring pucker is accompanied by rotation of the phenylacetyl moiety of the protein-bound penicillin. In this study, we explore the extent to which structure–activity correlation is shown in the topological details of the crystalline electron density, and whether evidence supporting the usual chemical concepts are reachable with current experimental methods and interpretive tools.

Penamecillin (**1**) and penamecillin-1β-sulfoxide (**2**) were chosen for an experimental charge-density study because **1** shows high antibacterial activity, whereas **2** does not; however, the compounds' structures differ only in the oxidation state of the thiazolidine sulfur atom.

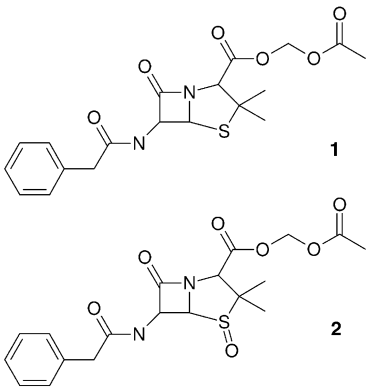

1

2

An earlier diffraction study[11] revealed no significant structural difference between compounds **1** and **2** with respect to the geometry and bonding situation of the β-lactam rings.

Experimental Section

Colorless crystals of penamecillin and penamecillin-1β-sulfoxide with dimensions of $0.30\times0.25\times0.25$ and $0.32\times0.25\times0.20$ mm^3, respectively, were measured at the beamline F1 of the storage ring DORIS III, at the HASYLAB/DESY in Hamburg. Wavelengths of 0.5606 and 0.5503 Å for the primary beam were used. The temperature was maintained at 100 K during the measurements by using an Oxford Cryosystems N_2-gas-stream cooling device. The CCD area detector was set to measure 51081 and 65555 reflections, up to a resolution of $\sin\theta/\lambda=1.23$ and 1.24 Å^{-1} (or $d=$ 0.40 Å), respectively. Penamecillin data for three different detector positions ($2\theta=0$, -30, and $-55°$) were collected. For the sulfoxide, two additional positions (30° and 55°) were used to increase the redundancy of the data. To prevent the very strong low-order reflections from exceeding the dynamic range of the CCD camera, the primary beam was weakened by 3 mm Al and 1 mm Al for **1** and **2**, respectively. The measurement strategy was planned with the program ASTRO,[12] the data collection was monitored with SMART,[12] and the frames were integrated and corrected with SAINT.[12] For scaling and merging, the program SORTAV[13] was used. Further details of the crystal data and the experimental conditions are given in Table 1.

CCDC-216531 and CCDC-216532 contain the supplementary crystallographic data for this paper. These data can be obtained free of charge via www.ccdc.cam.ac.uk/conts/retrieving.html (or from the Cambridge Crystallographic Data Centre, 12 Union Road, Cambridge CB2 1EZ, UK; fax: (+44) 1223-336-033; or e-mail: deposit@ccdc.cam.ac.uk).

Table 1. Crystallographic data for penamecillin (**1**) and penamecillin-1β-sulfoxide (**2**).

	1	**2**
empirical formula	$C_{19}H_{22}N_2O_6S$	$C_{19}H_{22}N_2O_7S$
M_r [g mol^{-1}]	406.46	422.46
crystal system	monoclinic	monoclinic
space group	$P2_1$ (No. 4)	$C2$ (No. 5)
Z	2	4
T [K]	100 (1)	100 (1)
a [Å]	12.830(3)	23.887(5)
b [Å]	7.937(2)	7.6533(15)
c [Å]	10.017(2)	12.435(3)
$\alpha=\gamma$ [°]	90.0	90.0
β [°]	104.67(3)	118.36(3)
V [Å^3]	986.7(4)	2000.4(9)
ρ [g cm^{-3}]	1.368	1.403
$F(000)$	428	888
μ [mm^{-1}]	0.11	0.11
crystal size [mm]	$0.30\times0.25\times0.25$	$0.32\times0.25\times0.20$
λ [Å]	0.5606	0.5503
max. 2θ [°]	87.48	86.20
$(\sin\theta/\lambda)_{max}$ [Å^{-1}]	1.23	1.24
index ranges	$-31\le h\le30$	$-59\le h\le51$
	$0\le k\le19$	$0\le k\le18$
	$0\le l\le24$	$0\le l\le30$
reflections collected	51081	65555
unique reflections	13926	16133
observed reflections [$F_o>2.5\sigma(F_o)$]	11991	12688
completeness [%]	86.5	96.9
R_{int}	0.036	0.050
parameters	543	577
$R(F)$ [%]	2.48	2.64
$R_w(F)$ [%]	2.55	2.81
GoF	1.20	0.87

Theoretical calculations: Single-point ab initio calculations for the experimental geometry at the Hartree–Fock (HF) and density functional (B3LYP) level of theories were completed by using the Gaussian 98[14] program package. The topology of the electron densities based on the 6-311++G(3df,3pd) and 6-311G(d,p) standard basis sets were analyzed by using the AIMPAC program.[15] The theoretical electrostatic potentials were directly derived by employing the Gaussian 98 program.

Multipole refinements: The conventional spherical atom refinement was performed by using the SHELXL-97[16] program to establish the starting positional and displacement parameters for the subsequent aspherical atom analysis. This was based on the Hansen–Coppens multipole formalism[17] implemented in the XD program package.[18] In all refinements the quantity $\Sigma_H w_H(|F_o(H)|-k|F_c(H)|)^2$ was minimized by using the statistical weight $w_H=\sigma(F_o(H))^{-2}$, and only those structure factors which met the criterion $F_o(H)>2.5\sigma(F_o(H))$ were included.

The same density model, including local symmetries and chemical constraints, was applied to both penicillin derivatives. Two types of oxygen atoms (carbonyl and ether) and four types of carbon atoms (methyl, methylene, phenyl, and those of the ring system) were modeled independently. Local site symmetry was applied as follows: For the carbon atoms C2, C12, C15, C21, C23, and all oxygen atoms except O9, local mirror symmetry was used. An *mm*2 symmetry was applied to the phenyl carbon atoms and 3*m* symmetry to the methyl groups. All non-hydrogen atoms were treated up to the hexadecapolar level of expansion, while a bond-directed dipole was introduced for the hydrogen atoms. The C–H and N–H distances were adjusted to average values provided by neutron diffraction analyses.[19] The parameters of the radial functions were deduced from single-zeta Hartree–Fock calculations on isolated atoms.[20] For the sulfur atom, radial parameters were derived by using multipole modeling of theoretical scattering factors based on the B3LYP6-311G(3df,3dp) density level of the chemically related thiazolidine-4-carboxylic acid molecule. The analysis of the simulated data led to the attainment of expansion–contraction parameters (κ_l) of the deformation radial functions for the bound sulfur atom. This approach has recently

been introduced to reduce inadequacies related to the radial functions of the multipole model and has led to considerable improvements in topological indices of bonds formed by first-row elements.[21] Further details of the refinement are summarized in Table 1.

Results and Discussion

The geometrical structural parameters found in the study by Labischinski et al.[11] can be confirmed by the low-temperature measurements. ORTEP[22] plots including the chosen atomic-numbering scheme are shown in Figure 1. The β-lactam rings of the two penicillin derivatives show similar features in that both are almost planar and the torsion angles C5-C6-C7-N4 are small with −8.03(4)° and −10.04(4)° for **1** and **2**, respectively. The C7−N4 bond length is only slightly shorter (by ~0.013 Å) in **1** than in **2**. The five-membered thiazolidine rings show an envelope conformation in both compounds, however, in penamecillin the atoms S1, C2, N4, and C5 are almost coplanar with C3 out-of-plane, whereas S1 is out-of-plane in the 1β-sulfoxide. As a consequence, the ester group is axial in **1** and equatorial in **2**. Further discussions on structural parameters can be found in the Labischinski paper.[11]

Interpretation of the charge-density distribution in terms of Bader's quantum theory of atoms in molecules (AIM)[23] allows the comparison of the two penicillin derivatives at the electron-density level. In Table 2, bond topological parameters based on the multipole models and several theoretical calculations of the lactam amide bonds are compared. The density at the bond critical point ($\rho(\boldsymbol{r}_b)$, a measure of charge accumulation and thus bond strength) is almost identical for both amide bonds in both compounds, irrespective of the method it is derived by. In contrast, the experimental Laplacian ($\bigtriangledown^2\rho(\boldsymbol{r}_b)$, a measure of charge concentration) is lower in value than that obtained from the wave function. The rather high ellipticity can be taken as an indication of

Table 2. The topology of the β-lactam bond C7−N4. Comparison of experimental and theoretical values of $\rho(\boldsymbol{r})$ and $\bigtriangledown^2\rho(\boldsymbol{r})$ at the bond critical point (BCP, located at $\boldsymbol{r}$, in which $\bigtriangledown\rho(\boldsymbol{r}_b)=0$), and the ellipticity ($\varepsilon$, defined by $\varepsilon=\frac{\lambda_1}{\lambda_2}-1$, in which λ_1 and λ_2 are the two principal curvatures of $\rho(\boldsymbol{r})$ at a BCP), a measure of the charge asphericity.

	Bond length [Å]	ρ [e Å^{-3}]	$\bigtriangledown^2\rho$ [e Å^{-5}]	ε
penamecillin				
multipole	1.3829(8)	2.20(5)	−17.2(2)	0.21
B3LYP6-311++G(d,p)		2.10	−21.4	0.10
B3LYP6-311++G(3df,3pd)		2.15	−23.8	0.14
penamecillin-1β-sulfoxide				
multipole	1.3955(7)	2.20(6)	−16.5(3)	0.25
B3LYP6-311++G(d,p)		2.05	−20.7	0.10
B3LYP6-311++G(3df,3pd)		2.10	−22.9	0.14
HF/6-311++G(3df,3dp)		2.16	−27.9	0.06

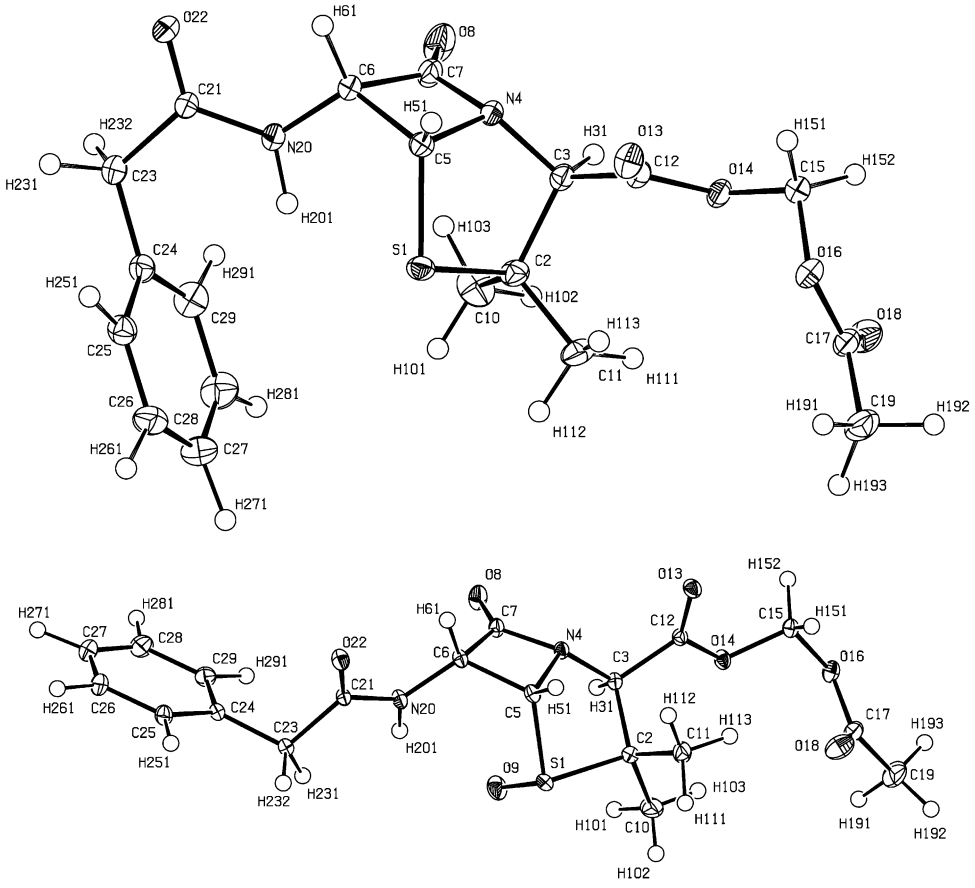

Figure 1. ORTEP[22] representation (50% probability) and atom-numbering scheme for penamecillin (above) and penamecillin-1β-sulfoxide (below).

the partial double-bond character and the strained β-lactam ring. In both compounds, however, the endocyclic amide bond appears to be weaker than the exocyclic one. The comparison of the above topological indices to those derived for peptide bonds in different dipeptides also suggests that the lactam amide bond is not a typical peptide bond (Table 3).

Table 3. Comparison of the topology of the β-lactam bond C7–N4 with different peptide bond values taken from the literature.

Bond	Bond length [Å]	ρ [e Å^{-3}]	$\nabla^2\rho$ [e Å^{-5}]	ε
penamecillin				
C7–N4	1.3829(8)	2.20(5)	−17.2(2)	0.21
C21–N20	1.3542(6)	2.34(5)	−23.0(2)	0.14
penamecillin-1β-sulfoxide				
C7–N4	1.3955(7)	2.20(6)	−16.5(3)	0.25
C21–N20	1.3587(6)	2.42(6)	−23.2(3)	0.15
cyclo-(D,L-Pro)-(L-Ala) monohydrate[3]	1.345(10)	2.45(3)	−23.7(21)	0.19(5)
average value from ref. [26]	1.338(5)	2.4(1)	−23.4(32)	0.21(8)
glycyl-L-threonine[27]	1.3403(3)	2.33(3)	−19.3(1)	0.44
N-acetyl-L-cysteine[28]	1.3402(4)	2.46(4)	−30.1(2)	0.24
DL-alanylmethionine[29]	1.3381(5)	2.32	−21.8	0.21

Based on the local topology of the density, the S1–C2 bond is somewhat weaker than the S1–C5 bond in both derivatives. However, more charge accumulation is seen in both bonds of **2** compared with **1**, in spite of the longer bond lengths of **2** (Table 4).

The Laplacian of the charge density, which is indicatative of regions of charge accumulation ($\nabla^2\rho(\boldsymbol{r})<0$) and charge depletion ($\nabla^2\rho(\boldsymbol{r})>0$), is displayed in Figure 2 as a volume-rendering representation of the two molecules. Compared with isosurface plots, volume rendering has the advantage that continuous regions of the Laplacian can be visualized. Until now, such representations were only available for theoretical Laplacian functions.[24] The different colors in Figure 2 represent different levels of the Laplacian, and the interval for which the Laplacian is displayed ranges from −25 to +25 e Å^{-5}. Both molecules are shown in a projection with the β-lactam and the phenyl rings clearly visible. In the core regions, the highly accumulated charge is indicated in white, red colors show the accumulation in the bonds, and blue halos around the electronegative oxygen denote charge depletion around the atoms.

Table 4. Experimental values of the electron density $\rho(\boldsymbol{r})$ and the Laplacian $\nabla^2\rho(\boldsymbol{r})$ at the bond critical points of the endocyclic and exocyclic bonds in the two penicillin derivatives.

Bond	Penamecillin		Penamecillin-β-sulfoxide	
	ρ [e Å^{-3}]	$\nabla^2\rho$ [e Å^{-5}]	ρ [e Å^{-3}]	$\nabla^2\rho$ [e Å^{-5}]
S(1)–C(2)	1.03(1)	−0.9(1)	1.18(2)	−5.9(1)
S(1)–C(5)	1.21(3)	−3.7(1)	1.24(3)	−4.6(1)
S(1)–O(9)	–	–	2.41(7)	−22.1(1)
C(7)–O(8)	3.06(7)	−35.5(4)	3.18(9)	−32.0(4)
C(3)–N(4)	1.94(5)	−10.3(2)	1.82(5)	−9.6(2)
C(5)–N(4)	1.92(4)	−13.1(2)	1.92(5)	−12.2(2)
C(7)–N(4)	2.20(5)	−17.2(2)	2.20(6)	−16.5(3)
C(6)–N(20)	2.00(5)	−14.2(2)	1.73(5)	−4.7(2)
C(2)–C(10)	1.58(3)	−7.2(1)	1.75(3)	−11.4(1)
C(2)–C(11)	1.57(1)	−7.2(1)	1.71(1)	−10.9(1)
C(2)–C(3)	1.47(4)	−9.7(1)	1.48(5)	−7.2(1)
C(3)–C(12)	1.93(4)	−16.1(1)	1.61(4)	−9.2(1)
C(5)–C(6)	1.56(4)	−9.1(1)	1.37(5)	−5.2(2)
C(6)–C(7)	1.76(4)	−11.2(1)	1.69(4)	−9.5(2)

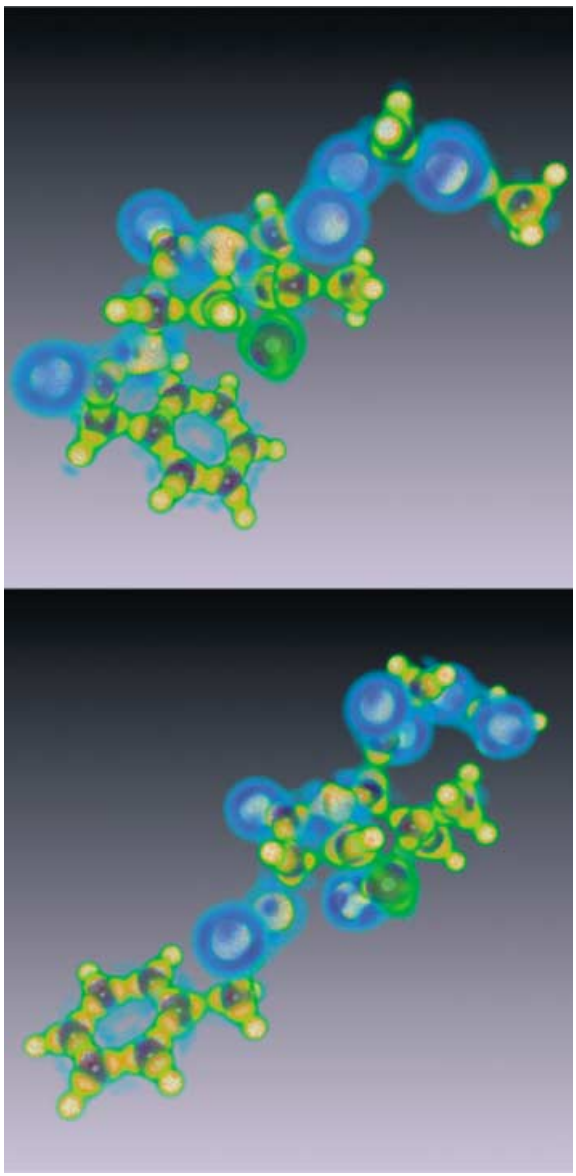

Figure 2. Volume-rendering representation of the Laplacian function of penamecillin (above) and penamecillin-1β-sulfoxide (below). Blue colors denote positive values. Negative values are from green, orange, and red to white.

The oxidation of the sulfur atom in the sulfoxide yields an intramolecular hydrogen bond S1–O9···H201–N20. However, with a H–O distance of 2.23 Å and an electron density of 0.09(1) e Å^{-3} ($\nabla^2\rho(\boldsymbol{r})=1.4$ e Å^{-5}) at the bond critical point, it is a rather weak hydrogen bond. Nevertheless, due to this interaction the transition state for the opening of the β-lactam ring in the inactive sulfoxide might be unfavored.[10]

The electrostatic potential represents regions in which a positive test charge is attracted (negative potential) and repelled (positive potential). Figure 3 shows isosurfaces of the

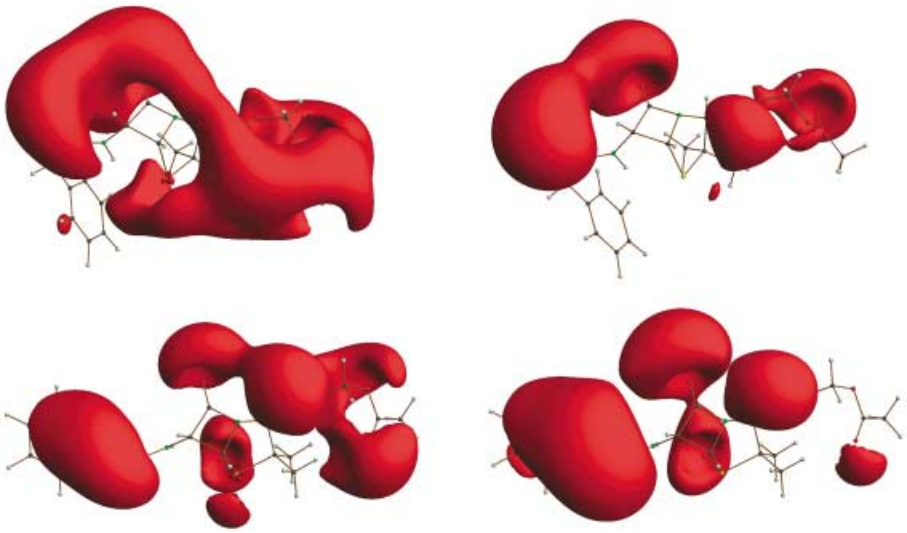

Figure 3. Top: Electrostatic potentials of penamecillin (isosurfaces with $V_{EP} = -0.05$ e Å^{-1}). Bottom: Electrostatic potentials of penamecillin-1β-sulfoxide (isosurfaces with $V_{EP} = -0.05$ e Å^{-1}). For both, the multipole model is shown on the left and the B3LYP6-311++G(d,p) density on the right.

negative electrostatic potential (EP) obtained from the experimental charge density, following the method developed by Su and Coppens[25] and from quantum chemical calculations. The major features are alike, but for both compounds the experimental EP is more extended. The reason for this is that the experimental EP corresponds to a molecule extracted from the crystal and includes all inductive and polarization effects of the environment, whereas the theoretical EP refers to isolated molecules. An interesting observation that might have a chemical significance is the difference in spatial distribution of the negative EP around the ring system in the two compounds. Whereas the carbonyl carbon atom (C7) is reachable from above the ring in both compounds, a nucleophilic attack from the opposite side is possible only in the active penamecillin; this side is blocked by a negative potential caused mainly by the oxidized sulfur atom in the inactive 1β-sulfoxide. Another crucial feature of the EP of **2**, which is lacking in the active compound, is the negative lobes around the phenyl ring. This discrepancy cannot be attributed to crystal-field effects because theoretical calculations on the isolated molecule yield very similar results.

Conclusion

The results of this charge-density study support the conventional interpretation that relates penicillin activity to the weak lactam amide bond; less/more charge is both accumulated and concentrated in the C7–N4/C7–O8 bond than that characteristic of the related bonds in peptide moieties. While no clear evidence for the activity difference was found in terms of the local topology of these bonds, all neighbouring bonds appear to possess more covalent character in the active compound than in the inactive compound. This extra stability of the lactam ring of **1** cannot be attributed to conformational differences. Features that are not directly evident from the analysis of the electron density become apparent in the EP, which is significantly different for the two penicillins. In the inactive derivative, the site of nucleophilic attack is shielded by a region of negative potential extending over one side of the lactam ring. This blocking of the carbonyl bond can be an important contribution to the inactivity of **2** if the conformation of the penam ring is preserved upon binding to the active site of the enzyme. The intramolecular S1–O9···H201–N20 hydrogen bond interaction is of special importance in this respect because it gives an additional contribution to stabilize the ring framework. An interesting observation is that the phenylalanyl residue in **2** is strongly polarized, as indicated by the negative EP that is extended over both sides of the phenyl ring. This feature is completely missing for compound **1** in which the opposite end of the molecule is found to be more polarized. Although the significance of this observation is not clear to us, the results suggest that the phenyl terminus can play an unusual role in recognition. We think that this and similar studies can contribute to our understanding of molecular processes in biochemical systems, mainly because experimentally derived electronic properties include effects of intermolecular interactions. Recent technical developments have made it possible to carry out experimental charge-density work on larger molecules, in a reasonable time period, and even allow for comparative studies on a series of biologically related molecules. This method certainly has the potential of yielding information far beyond the usual atomic connectivity.

[1] C. Jelsch, M. M. Teeter, V. Lamzin, V. Pichon-Pesme, R. H. Blessing, C. Lecomte, *Proc. Natl. Acad. Sci. USA* **2000**, *97*, 3171.
[2] A. Wagner, R. Flaig, D. Zobel, B. Dittrich, P. Bombicz, M. Strümpel, P. Luger, T. Koritsánszky, H.-G. Krane, *J. Phys. Chem. A* **2002**, *106*, 6581.
[3] B. Dittrich, T. Koritsánszky, M. Grosche, W. Scherer, R. Flaig, A. Wagner, H.-G. Krane, H. Kessler, C. Riemer, A. M. M. Schreurs, P. Luger, *Acta Crystallogr. Sect. B* **2002**, *58*, 721.
[4] X. Li, G. Wu, Y. A. Abramov, A. V. Volkov, P. Coppens, *Proc. Natl. Acad. Sci. USA* **2002**, *99*, 12132.
[5] T. Koritsánszky, R. Flaig, D. Zobel, H.-G. Krane, W. Morgenroth, P. Luger, *Science* **1998**, *279*, 356.
[6] D. J. Waxman, J. L. Strominger, *Annu. Rev. Biochem.* **1983**, *52*, 825.
[7] R. M. Sweet, *Cephalosporins and Penicillins; Chemistry and Biology*, Academic Press, New York, **1972**.
[8] N. V. Joshi, R. Virudachalam, V. S. R. Rao, *Curr. Sci.* **1978**, *47*, 933.
[9] N. C. Cohen, *J. Med. Chem.* **1983**, *26*, 259.
[10] C. E. McVey, M. A. A. Walsh, G. G. Dodson, K. S. Wilson, J. A. Brannigan, *J. Mol. Biol.* **2001**, *313*, 139.
[11] H. Labischinski, D. Naumann, G. Barnickel, W. Dreißig, W. Gruszecki, A. Hofer, H. Bradaczek, *Z. Naturforsch. B* **1987**, *42*, 367.

[12] ASTRO (1995–1996), SMART (1996), SAINT (1994–1996), Bruker AXS, Inc., Madison, Wisconsin, USA.
[13] R. H. Blessing, *J. Appl. Crystallogr.* **1997**, *30*, 421.
[14] *Gaussian 98*, Revision A.7, M. J. Frisch, G. W. Trucks, H. B. Schlegel, G. E. Scuseria, M. A. Robb, J. R. Cheeseman, V. G. Zakrzewski, J. A. Montgomery, Jr., R. E. Stratmann, J. C. Burant, S. Dapprich, J. M. Millam, A. D. Daniels, K. N. Kudin, M. C. Strain, O. Farkas, J. Tomasi, V. Barone, M. Cossi, R. Cammi, B. Mennucci, C. Pomelli, C. Adamo, S. Clifford, J. Ochterski, G. A. Petersson, P. Y. Ayala, Q. Cui, K. Morokuma, D. K. Malick, A. D. Rabuck, K. Raghavachari, J. B. Foresman, J. Cioslowski, J. V. Ortiz, B. B. Stefanov, G. Liu, A. Liashenko, P. Piskorz, I. Komaromi, R. Gomperts, R. L. Martin, D. J. Fox, T. Keith, M. A. Al-Laham, C. Y. Peng, A. Nanayakkara, C. Gonzalez, M. Challacombe, P. M. W. Gill, B. G. Johnson, W. Chen, M. W. Wong, J. L. Andres, M. Head-Gordon, E. S. Replogle, J. A. Pople, Gaussian, Inc., Pittsburgh, PA, **1998**.
[15] J. Cheeseman, T. A. Keith, R. W. F. Bader, AIMPAC program package, McMaster University, Hamilton, Ontario, Canada, **1992**.
[16] G. M. Sheldrick, SHELXL-97, *Program for Refinement of Crystal Structures*, University of Göttingen, Germany, **1997**.
[17] N. K. Hansen, P. Coppens, *Acta Crystallogr. Sect. A* **1978**, *34*, 909.
[18] T. Koritsánszky, S. Howard, T. Richter, Z. W. Su, P. R. Mallinson, N. K. Hansen, XD, *Computer Program Package for Multipole Refinement and Analysis of Electron Densities from Diffraction Data*, User manual, Freie Universität Berlin, Germany, **1995**.
[19] F. H. Allen, O. Kennard, D. G. Watson, L. Brammer, A. G. Orpen, R. Taylor, *International Tables for Crystallography, Vol. C*, Kluwer Academic Publishers, Amsterdam, **1992**, Chapter 9.5, pp. 685–706.
[20] E. Clementi, C. Roetti, *At. Data Nucl. Data Tables* **1974**, *14*, 177.
[21] A. Volkov, Y. Abramov, P. Coppens, *Acta Crystallogr. Sect. A* **2001**, *57*, 272.
[22] M. N. Burnett, C. K. Johnson, ORTEP-III, *Oak Ridge Thermal Ellipsoid Plot Program for Crystal Structure Illustrations*, Oak Ridge National Laboratory Report ORNL-6895, Oak Ridge, Tennessee, USA, **1996**.
[23] R. F. W. Bader, *Atoms in Molecules: A Quantum Theory*, Clarendon Press, Oxford, **1990**.
[24] P. J. MacDougall, C. E. Henze, *Theor. Chem. Acc.* **2001**, *105*, 345.
[25] Z. Su, P. Coppens, *Acta Crystallogr. Sect. A* **1992**, *48*, 188.
[26] V. Pichon-Pesme, H. Lachekar, M. Souhassou, C. Lecomte, *Acta Crystallogr. Sect. B* **2000**, *56*, 728.
[27] B. Dittrich, R. Flaig, T. Koritsánszky, H.-G. Krane, W. Morgenroth, P. Luger, *Chem. Eur. J.* **2000**, *6*, 2582.
[28] H.-P. Nabein, Diploma thesis, Freie Universität Berlin, Germany, January **2001**.
[29] R. Guillot, N. Muzet, S. Dahaoui, C. Lecomte, C. Jelsch, *Acta Crystallogr. Sect. B* **2001**, *57*, 567.

Received: October 15, 2003

Published online: April 28, 2004

